

RESEARCH ARTICLE

Use of standard U-bottom and V-bottom well plates to generate neuroepithelial embryoid bodies

David Choy Buentello^{1,2,3}, Lena Sophie Koch³, Grissel Trujillo-de Santiago^{1,4}, Mario Moisés Alvarez^{1,2*}, Kerensa Broersen^{3*}

1 Centro de Biotecnología-FEMSA, Tecnológico de Monterrey, Monterrey, NL, México, **2** Departamento de Bioingeniería, Tecnológico de Monterrey, Monterrey, NL, México, **3** Department of Applied Stem Cell Technologies, TechMed Centre Enschede, University of Twente, Enschede, The Netherlands, **4** Departamento de Ingeniería Mecatrónica y Eléctrica, Tecnológico de Monterrey, Monterrey, NL, México

These authors contributed equally to this work.

* mario.alvarez@tec.mx (MMA); k.broersen@utwente.nl (KB)



OPEN ACCESS

Citation: Choy Buentello D, Koch LS, Trujillo-de Santiago G, Alvarez MM, Broersen K (2022) Use of standard U-bottom and V-bottom well plates to generate neuroepithelial embryoid bodies. PLoS ONE 17(5): e0262062. <https://doi.org/10.1371/journal.pone.0262062>

Editor: Xiaoping Bao, Purdue University, UNITED STATES

Received: December 15, 2021

Accepted: April 8, 2022

Published: May 10, 2022

Copyright: © 2022 Choy Buentello et al. This is an open access article distributed under the terms of the [Creative Commons Attribution License](https://creativecommons.org/licenses/by/4.0/), which permits unrestricted use, distribution, and reproduction in any medium, provided the original author and source are credited.

Data Availability Statement: All relevant data are within the paper and its [Supporting Information](#) files.

Funding: This work was financially supported by the Netherlands Organ-on-Chip Initiative (NOCI) and By NWO (Dutch Research Council) – Gravity and Alzheimer Nederland grants. DCB thankfully acknowledge the financial support of Consejo Nacional de Ciencia y Tecnología (CONACyT) in the form of a doctoral scholarship. GTdS and MMA gratefully acknowledge the financial support from

Abstract

The use of organoids has become increasingly popular recently due to their self-organizing abilities, which facilitate developmental and disease modeling. Various methods have been described to create embryoid bodies (EBs) generated from embryonic or pluripotent stem cells but with varying levels of differentiation success and producing organoids of variable size. Commercial ultra-low attachment (ULA) V-bottom well plates are frequently used to generate EBs. These plates are relatively expensive and not as widely available as standard concave well plates. Here, we describe a cost-effective and low labor-intensive method that creates homogeneous EBs at high yield in standard V- and U-bottom well plates by applying an anti-adherence solution to reduce surface attachment, followed by centrifugation to enhance cellular aggregation. We also explore the effect of different seeding densities, in the range of 1 to 11×10^3 cells per well, for the fabrication of neuroepithelial EBs. Our results show that the use of V-bottom well plates briefly treated with anti-adherent solution (for 5 min at room temperature) consistently yields functional neural EBs in the range of seeding densities from 5 to 11×10^3 cells per well. A brief post-seeding centrifugation step further enhances EB establishment. EBs fabricated using centrifugation exhibited lower variability in their final size than their non-centrifuged counterparts, and centrifugation also improved EB yield. The span of conditions for reliable EB production is narrower in U-bottom wells than in V-bottom wells (i.e., seeding densities between 7×10^3 and 11×10^3 and using a centrifugation step). We show that EBs generated by the protocols introduced here successfully developed into neural organoids and expressed the relevant markers associated with their lineages. We anticipate that the cost-effective and easily implemented protocols presented here will greatly facilitate the generation of EBs, thereby further democratizing the worldwide ability to conduct organoid-based research.

CONACyT (SNI scholarships 26048 and 256730) and the Biocodex Foundation, México. The funders had no role in study design, data collection and analysis, decision to publish, or preparation of the manuscript.

Competing interests: The authors have declared that no competing interests exist.

Introduction

Embryoid bodies (EBs) have garnered great interest in recent years as a powerful tissue engineering platform due to their self-reproducing and multipotent differentiation capabilities. EBs are precursors to organoids, whose self-organizing properties allow their exploitation as developmental and disease models [1–3]. While procedures exist for organoid differentiation, the success of the differentiation process relies heavily on the ability to control certain variables involved in the formation of EBs [4, 5]. For example, having a spherical form is a prerequisite for most EB protocols, as this standardizes the gradient profiles that contribute to homogeneity [6]. However, arguably, the most important parameter when considering successful organoid differentiation is the initial diameter of the EB itself. Variation in diameter size severely affects differentiation, as increases in diameter result in longer diffusion times, thereby reducing the number of cells in the inner parts of the EB that have immediate contact with nutrients and differentiation factors [7, 8]. Many traditional protocols cite EB diameter sizes ranging from 150 to 600 μm [9, 10]; however, these sizes are generally not standardized. Consequently, current protocols result in EBs exhibiting wide variability in their diameters (i.e., 50 μm and higher). Having better control of the initial cell aggregate diameter would improve the differentiation of EBs into functional organoids. Previous studies have shown differentiation yields greater than 90% with improved culture methods [11, 12]. A fabrication process that enhances EB homogeneity would also favor the faithful reproducibility of culture and differentiation trajectories.

Forcing the formation of EBs using chemical and geometric molds can attenuate these diameter discrepancies. For example, the traditional hanging drop method allows small clusters of cells to aggregate through gravitational forces [13]. However, hanging drop methods also have their limitations, as EBs fabricated by the hanging drop method are generally small in size, have a low differentiation yield, and are prone to bursting/disaggregation [14]. The use of concave molds facilitates the aggregation of cells in a high-throughput and reproducible manner [15], and several reports have illustrated the use of ad hoc lab-made molds to produce spheroids (in general) and EBs (in particular).

Nevertheless, the use of commercially available culture devices has advantages over custom-made devices in terms of availability, reproducibility, and even price. For this reason, V-bottom well plates have been used extensively for the formation of EBs since their introduction. Now, coupled with an ultra-low-adhesion (ULA) layer, V-bottom plates have become the standard for EB formation [16]. Stem cells are prone to attach to surfaces, so an ultra-low adhesion coating is needed to allow the formation of cellular aggregates in well plates [17, 18]. Therefore, the ULA V-bottom plates also enable a less labor-intensive EB fabrication and facilitate control over cellular aggregation [19, 20]. However, these plates are still not readily available and can be expensive.

A number of methods have been reported to treat regular culture wells with different solutions and materials (i.e., agar or a polyvinyl alcohol (PVA) solutions) to confer them with anti-adherent properties [16, 21]; however, these methods often involve multiple steps that can be cumbersome and time consuming. Here, we introduce and demonstrate the use of a cost-effective and rapid preparation method that imparts the ability to produce homogenous EBs at high yield and with a strong differentiation potential in conventional and commercially available non-ULA U-bottom and V-bottom well plates. Our method involves rinsing standard untreated tissue culture well plates with an anti-adherence solution 10 min before cell seeding, followed by centrifugation. This method is not resource-intensive and creates a hydrophobic surface that enhances cell aggregation in commercially available U- or V-bottom well plates for reliable formation of EBs that can efficiently differentiate into organoids.

Methods

Stem cell culture maintenance

The human embryonic stem cell (hESC) line H9 (WiCell, WA09) was obtained from the University of Leiden Medical Center. H9 cells were cultured at 37°C and 5% CO₂ in feeder-free conditions in Essential 8™ (E8 medium (Gibco, Life Technologies, cat. no. A1517001; Carlsbad, CA, USA) in cell culture dishes coated with 5 µg/mL Vitronectin (Gibco, cat. no. A31804; Carlsbad, CA, USA). The hESCs were subcultured with 0.5 mM ethylenediaminetetraacetic acid (EDTA) (Invitrogen, Life Technologies, cat. no. 15575020; Waltham, MA, USA) every 4 days to avoid overcrowding and exponential differentiation. The passage number was kept below 60, and the cultures were routinely checked for mycoplasma contamination. Pluripotency was ensured by evaluating the expression of the markers Oct3/4 and SOX2.

Well-plate coating

A 100 µL volume of anti-adherence rinsing solution (StemCell Technologies, cat. no. 07010; Canada) was added to untreated sterile CellStar U-bottom or V-bottom (Fig 1) 96-well plates (Greiner Bio-One, cat. no. 650185(U), 651161(V); Austria). After incubation for 5 min at room temperature, the anti-adherence rinsing solution was aspirated, and the wells were washed with Dulbecco's phosphate buffered saline (DPBS) (Gibco, cat. no. 14190250; Carlsbad, CA, USA) for another 5 min at room temperature. The DPBS was aspirated before cell seeding.

Embryoid body formation

For EB formation, a previously published protocol was adapted [10] (Fig 1). A single-cell suspension of hESCs was created by treatment of the cell culture with 0.5 mM EDTA for 3 min at

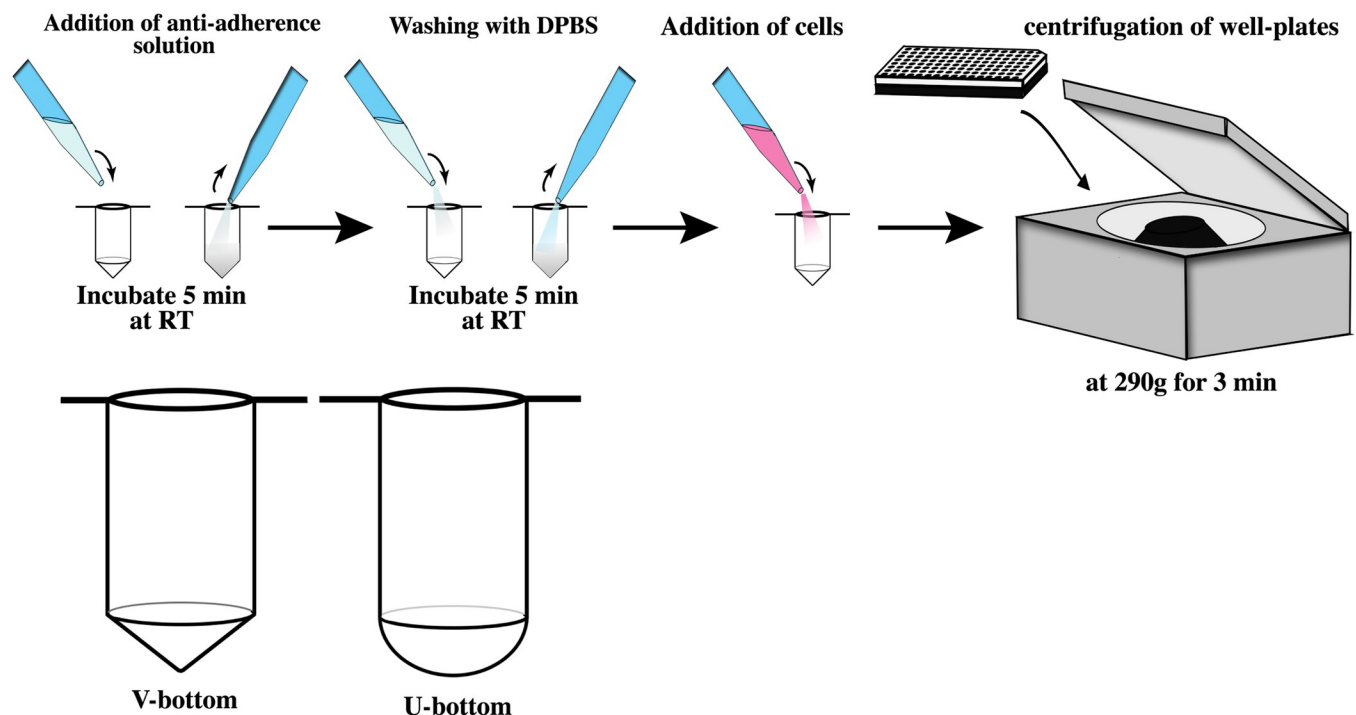


Fig 1. Protocol for embryoid body formation and different well geometries. We added anti-adherence solution into regular U- and V-bottom wells and incubated for 5 minutes at room temperature to develop anti-adherence coated plates and then washed gently with PBS. The application of an anti-adherence solution to conventional V-bottom and U-bottom plates enabled reproducible EB generation in low-cost well plates.

<https://doi.org/10.1371/journal.pone.0262062.g001>

room temperature. The released cells were collected, spun down, and counted. A range of 1,000–11,000 cells per well was seeded into wells prefilled with 150 μ L Essential 6™ (E6 medium) (Gibco, Carlsbad, CA, cat. no. A1516401; USA) supplemented with 10 μ M ROCK inhibitor (Selleckchem, cat. no. S1049; Houston, TX, USA). The anti-adherence coated well plates or the ultra-low attachment (ULA) 96-well plates (Corning, ref 7007; Kennebunk, ME, USA) well plates were then centrifuged at 290 \times g for 3 min and incubated at 37°C with 5% CO₂.

After 24 h, the culture medium was changed to E6 medium supplemented with 2 μ M XAV939 (Tocris Bioscience, Bristol, cat. no. 3748; UK), 10 μ M SB431542 (R & D Systems, cat. no. 1614/50; Minneapolis, MN, USA), and 500 nM LDN193189 (StemCell Technologies, cat. no. 72147; Canada). The culture medium was changed daily.

Microscopy and image analysis

Bright field images were collected every day using an EVOS cell imaging system (Thermo Fisher Scientific, Waltham, MA, USA). A 4 \times objective lens (16.0 mm working distance) was used for all images. Images were then imported into Adobe Photoshop CS6 (San Jose, CA, United States) for analysis. The EBs were isolated in the images by creating layer masks when contrasting an EB perimeter with its surroundings. The layer masks were smoothed using the “feather” function with a 5 pixels radius. Measurements (height, width area) and circularity were obtained using the “measurement” function of Photoshop.

Organoid differentiation

Brain (telencephalic) organoids were differentiated using a previously published protocol [22] with minor modifications. In brief, 50 μ L of Matrigel™ (3 mg/mL; Corning, cat. no. 356230; New York, NY, United States,) was added to the wells of an untreated 96-well flat-bottom plate to create a bed layer and allowed to set for 15 min at 37°C. EBs were then transferred to individual bed layers and covered with an additional 50 μ L of Matrigel to ensure full encapsulation of the EB. The top layer was allowed to set for another 15 min at 37°C, then differentiation medium was added. We conducted experiments of unguided and guided differentiation. In both cases, the basic differentiation medium consisted of Neurobasal-A (Gibco, Life Technologies, cat. no. 21103049; Carlsbad, CA, USA), 1 \times B27 without vitamin A (Gibco, Life technologies, cat. no. 17504044), 1 \times GlutaMax (Gibco, Life Technologies, cat. no. 35050038), and 1% (v/v) penicillin/streptomycin (Gibco, Life Technologies, cat. no.15070063). For unguided differentiation, the medium was supplemented with 20ng/mL of FGF-2 (Gibco, Life technologies, cat no. PHG0261) and 20ng/mL of EGF (Gibco, Life technologies, cat no. PHG0311L). For guided differentiation, the basic differentiation medium was added with 3 μ M CHIR99021 (Axon Medchem, cat. no. CT 99021; Reston, VA, USA) and 0.5 ng/mL bone morphogenic protein (BMP4, R & D Systems, cat. no. 314; Minneapolis, MN, USA). The medium was changed every other day. CHIR and BMP4 were only added for the first 3 days.

Image analysis and statistical analysis

The diameter of each EB was calculated using the average of the height and width of the spheroid. For comparison between variables, values were exported to Prism 8 (GraphPad, v 8.4.3; San Diego, CA, USA) for one-way analysis of variance (ANOVA) ($P < 0.001$) to establish significant differences. Five independent replicates were conducted for each EB fabrication treatment ($N = 5$). At least 5 spheroids were analyzed per treatment ($n = 5$) in each independent experiment.

EB viability assays

The Live/Dead™ assay (Invitrogen, Life Technologies, cat. no. L3224; Waltham, MA, USA) was used to determine the viability of EBs fabricated at different cell seeding densities in U-bottom or B-bottom wells. These assays were conducted after 6 days of culture according to the manufacturer's instructions. In brief, 2 μ M calcein AM (1:1000) and 4 μ M EthD-1 (1:500) working solutions were prepared in PBS. A 150 μ L volume of the working solutions was added to cover the EBs. The EBs were then incubated at room temperature for 45 min, the solution was aspirated, and the medium was replenished. The EBs were imaged immediately with a Zeiss (LSM880) confocal microscope using an FITC channel (for green fluorescence) and an EtHD1 channel (for red fluorescence). A z-stack of 20 fluorescence images (10 μ m apart on the z-axis) was rendered as a single image for analysis using ImageJ (NIH; Bethesda, MD, USA) and processed using the particle analysis tool. In the experiments to determine viability, at least 3 EBs were examined per treatment (n = 3).

Immunohistochemistry

After 30 days of culture, organoids were fixed in 4% formaldehyde for 60 min at room temperature, followed by an overnight incubation in 30% sucrose in PBS at 4°C. The organoids were then embedded in Shandon cryomatrix (ThermoFisher, cat. no. 6769006; Waltham, MA, USA), flash frozen at -80°C, and cut into 5 μ m sections using a cryostat (SLEE medical GmbH, type MNT; Germany). After an additional fixation step with acetone at 4°C, the sections were blocked with 1% BSA and 0.025% Triton-X 100 in PBS for 1 h at room temperature.

The sections were then incubated with primary antibodies (rabbit anti-MAP2, 1:200, Abcam, cat.no. ab32454; mouse anti-GFAP, 1:500, Abcam, cat.no. ab212398; mouse anti- β 3-tubulin, 1:500, Santa Cruz Biotechnology, cat.no. sc-80005) in blocking solution overnight at 4°C, followed by incubation with secondary antibodies and conjugated antibodies in blocking buffer (SOX2-GFP, 1:500, eBioscience, cat.no.53-9811-82; Donkey anti-mouse, AF647, ThermoFisher, cat. No. A31571, goat anti-rabbit AF594, Invitrogen, cat. No. R37117) for 1 h at RT. Nuclei were visualized with DAPI (ThermoFisher Scientific, cat.no. D1206) in PBS for 20 min.

The [terminal deoxynucleotidyl transferase](#) dUTP nick end labeling (TUNEL) assay was conducted using a commercially available TUNEL assay kit (BrdU-Red; Abcam, cat. No. ab66110; UK) according to the manufacturer's instructions. In brief, a 20 μ g/mL solution of proteinase K was prepared by combining 2 μ L of a stock proteinase K solution (10 mg/mL; Invitrogen, cat.no. 25530031), 998 μ L of Tris-HCl pH 8.0, and 50 mM EDTA. After acetone fixation, the sections were incubated for 5 min with 2 μ L of this prepared proteinase K solution, followed by a 5 min incubation with 4% formaldehyde and then two 5 min washes with the washing buffer included in the kit. The sections were then covered with the DNA labeling solution included in the kit (consisting of the reaction buffer, the terminal deoxynucleotidyl transferase [TdT] enzyme, and 5-bromo-2'-deoxyuridine 5'-triphosphate [BrdUTP]) and incubated for 1 h at 37°C. After washing to remove the DNA labeling solution, the sample was incubated in Anti-BrdU antibody solution (1:100) for 30 min at room temperature. The Anti-BrdU antibody is labeled with a red fluorochrome, and the BrdU-red signal was analyzed at Ex/Em 488/576 nm in a confocal microscope (LSM 880; Zeiss, Germany) equipped with an Airscan detector (SR, Zeiss; Germany).

The Fluoro-Jade assay was also conducted using a commercial kit (Fluoro-Jade C (FJC) ready-to-dilute staining kit for identifying degenerating neurons; Biosensis, Cat. No. AG 325; Australia). Briefly, the sections were fixed with acetone and incubated for 5 min with 2 μ L of the 20 μ g/mL proteinase K solution described above, followed by a 5 min incubation with 4%

formaldehyde, and then two 5 min washes with distilled water. After washing, the samples were incubated in the Fluoro-Jade (1:200) and DAPI (1:200) solutions for 30 min at room temperature. The samples were then rinsed three times (1 min each) in distilled water and observed under blue light excitation for Fluoro-Jade and UV light excitation for DAPI in a confocal microscope (LSM 880; Zeiss, Germany) equipped with an Airscan detector (SR, Zeiss; Germany).

FluoVolt signaling

Organoids were incubated with a voltage-sensitive dye (FluoVolt; Invitrogen, Cat. No. F10488), as instructed by the manufacturer. Briefly, organoids were treated with sterile normal saline solution (Intermountain, USP grade; Fisher Scientific; Waltham, MA, USA) supplemented with the dye (1:1000) and with the PowerLoad concentrate (1:100), for 45 min at room temperature. Time-lapse images were taken using a Zeiss microscope (LSM880; Zeiss, Germany) equipped with an Airyscan detector (SR; Zeiss, Germany) for fast image capture. Full area image scans were taken every 10 ms for 10 min. Fluorescence signals were processed using custom ImageJ (NIH; Bethesda, MD, USA) and MATLAB (MathWorks; Portola Valley, CA, USA) scripts.

Amyloid beta

Amyloid β ($A\beta$) was purified as previously reported [23]. Vials containing 0.5 mg $A\beta$ 40-HFIP films (rPeptide; cat. No.A-1153-1; Georgia, USA) were defrosted at room temperature for 10 min and dissolved in 500 mL hexafluoroisopropanol (HFIP) (Sigma, Germany, cat. 920-66-1) by vortexing vigorously for 1 min. The HFIP was removed by evaporation under a stream of nitrogen gas, and the $A\beta$ was redissolved in 500 mL dimethyl sulfoxide (DMSO). The $A\beta$ peptide solutions were then separated from the DMSO by passage through a desalting column (HiTrapTM desalting column; GE Healthcare, cat. 17-1408-01; Chicago, IL, USA) pre-equilibrated with 25 mL Tris-HCl buffer (50 mM Tris-HCl, 1 mM EDTA, pH 7.4). The $A\beta$ -containing samples were collected in pre-cooled, low-adhesion, resin-coated polypropylene centrifuge tubes (Bioplastics; cat. B74030; Netherlands). The $A\beta$ concentration was assessed using the Bradford assay for protein determination. Samples were kept on ice directly after elution, and any further experiments were conducted within 2 h after elution from the desalting column.

Results and discussion

Here, we demonstrated the use of standard, commercially available V-bottom and U-bottom well culture plates for the fabrication of functional neural EBs from human embryonic stem cells. Stem cells have a strong tendency to adhere to surfaces; therefore, we added a commercial anti-adherence solution to inhibit cell adhesion to the surface of wells and instead to favor cell aggregation. We also explored the use of a centrifugation step to further promote cell aggregation. Furthermore, we showed that the use of different initial cell seeding densities yielded EBs of different final diameters, thereby offering a way to precisely define and customize the size of neural EBS. This protocol yielded functional EBs that successfully differentiated into neural organoids.

Our integration of the use of a commercially available anti-adherence solution and a short centrifugation step resulted in a cost-effective and reproducible protocol for neural EB fabrication that can use conventional, readily available U- and V-bottom plates. The methods presently available for fabricating neural spheroids and EBs frequently depend on the use of ULA plates (both U- and V-bottom shaped) [24–26], which are more expensive and therefore less available than standard plates.

Our hESC culture system produced EBs after 6 days of culture. The EBs exhibited a characteristic neuroepithelial development, including a translucent body with a bright surface and smooth edges (S1A and S1B Fig) [10]. We used these (morphological) attributes for our initial assessments and to ensure the quality of EB formation. We found that EBs showing grainy, bumpy, or fading edges tended not to survive until the end of induction (day 6) (S1C Fig).

Cells in untreated well plates usually formed a central cluster, with small satellite aggregates along the slope of the well plate (S1C Fig). We did not observe reproducible formation of consolidated tissue in wells not treated with the non-adherence solution. By contrast, most cells precipitated into a singular cluster in the treated wells (S1A and S1B Fig). Aggregation seemed to be positively correlated with survivability, as none of the EBs cultured in untreated well plates survived beyond the first couple of days. The inability to form single clusters resulted in loose cellular interactions and loss of the desired round EB shape. This presumably led to cell death and aggregate fragmentation (S1C Fig).

Effects of seeding density and geometry on EB size and shape

Fig 2A shows the evolution of size in the EBs formed and cultured in U-bottom plates at different initial seeding conditions, with or without well centrifugation. Fig 2B shows the size evolution of EBs cultured in V-bottom wells and derived from different initial cell counts per well. Trends associated with centrifuged and non-centrifuged plates are also compared. As expected, higher seeding densities (i.e., the number of cells seeded per well at the initial time point) resulted in higher initial and final diameters.

The EB diameter is influenced by the seeding concentration [27]. In our experiments, an increase in the diameter of the EBs during 6 days of culture was also a function of the initial cell density. In general, we observed an average increase of nearly 100 μm in the diameter of EBs formed at high initial cell densities (i.e., 9×10^3 and 11×10^3 cells per well). The EBs formed in the wells initially seeded with 5×10^3 and 7×10^3 cells per well showed an increase in diameter of nearly 75 μm , while the EBs formed at the lowest initial cell density of 3×10^3 cells per well increased their diameter only modestly during the 6 days of culture. However, under equal seeding conditions, we did not observe significant differences between the average initial or final diameters of EBs when the cells were centrifuged or not centrifuged in the well systems (except for seeding densities of 9×10^3 and 11×10^3 cells per well).

Consistent with previous reports [28, 29], our results suggest that the geometry of the well affects the process of EB formation. The V-bottom wells created EBs with a slightly larger (but not statistically significant) initial diameter than their U-bottom counterparts (Fig 2A and 2B). However, we observed clear differences in the final diameters of EBs formed in U-bottom versus V-bottom plates, as the EBs formed in V-bottom wells were significantly larger (Figs 2B and 3A). For example, EBs cultured for 6 days in U-bottom or V-bottom wells exhibited an average diameter of 429 ± 12 and 511 ± 40 μm , respectively (Fig 3A). Notably, the EBs generated in U-bottom plates only reached 500 μm in diameter at the highest seeding densities (i.e., 11×10^3 cells per well) and with the assistance of the centrifugation step. The increase in diameter of the EBs from their initial size was also lower in U-bottom than in V-bottom plates. These observations can be explained using geometrical arguments, as V-bottom wells have concave bottoms with a steeper slope than U-bottom wells and therefore have a larger initial diameter. This means that more cells are able to precipitate to form larger agglomerates in V-bottom plates. Indeed, we observed that some cells remained floating in the culture medium in the rounder U-bottom wells and were not integrated to the main EB (S1 Fig. Ciii).

Fig 3A shows the average diameters achieved in all our EB-fabrication experiments. The largest EBs were obtained with V-bottom wells and centrifugation. Interestingly, the formation

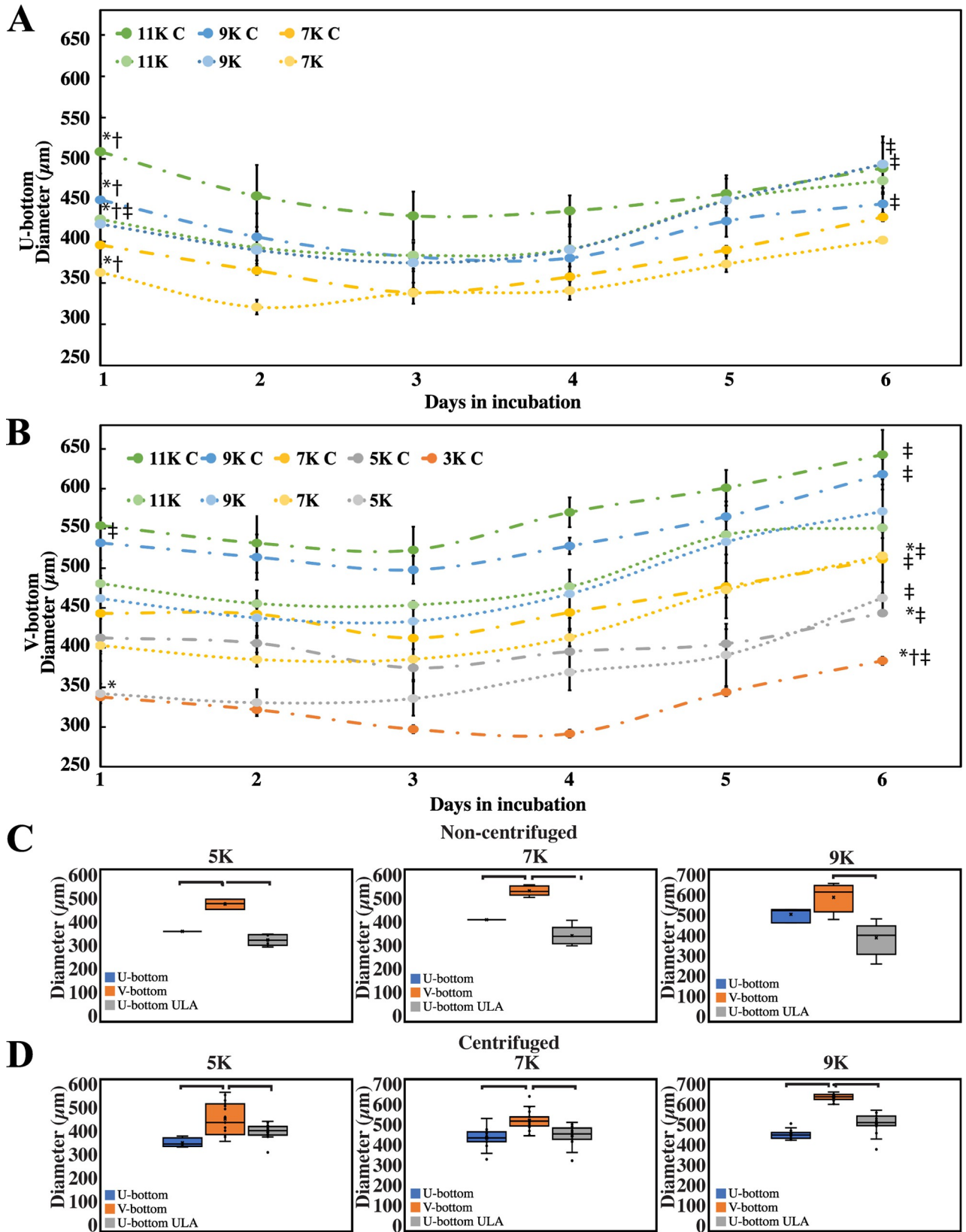


Fig 2. Characterization of embryoid body (EB) quality and daily growth. (A) The graphs depict EBs diameter in U-bottom wells coated with anti-adherence solution. (B) EB growth progression cultured in V-bottom wells coated with anti-adherence solution. Graphs shows different color-coded seeding concentrations given in thousands ("K") and if centrifuged ("C"). * $P < 0.001$ indicates a significant difference for all EBs of the same well plate and centrifugation. † $P < 0.001$ indicates a significant difference for EBs of the same well plate type but different centrifugation condition. ‡ $P < 0.001$ indicates a significant difference for EBs with different plate types but the same centrifugation condition. Scale bar: 200 μm . We considered at least 5 EBs ($n = 5$) for each experimental group at the beginning of the experiment, and we conducted 5 independent experiments ($N = 5$).

<https://doi.org/10.1371/journal.pone.0262062.g002>

experiments in V-bottom wells indicated that the use of a centrifugation step has a clear effect only with high seeding densities (i.e., 9×10^3 and 11×10^3 cells per well). Fig 3A also shows the conditions that were most suitable for EB formation using U-bottom wells. In the absence of a

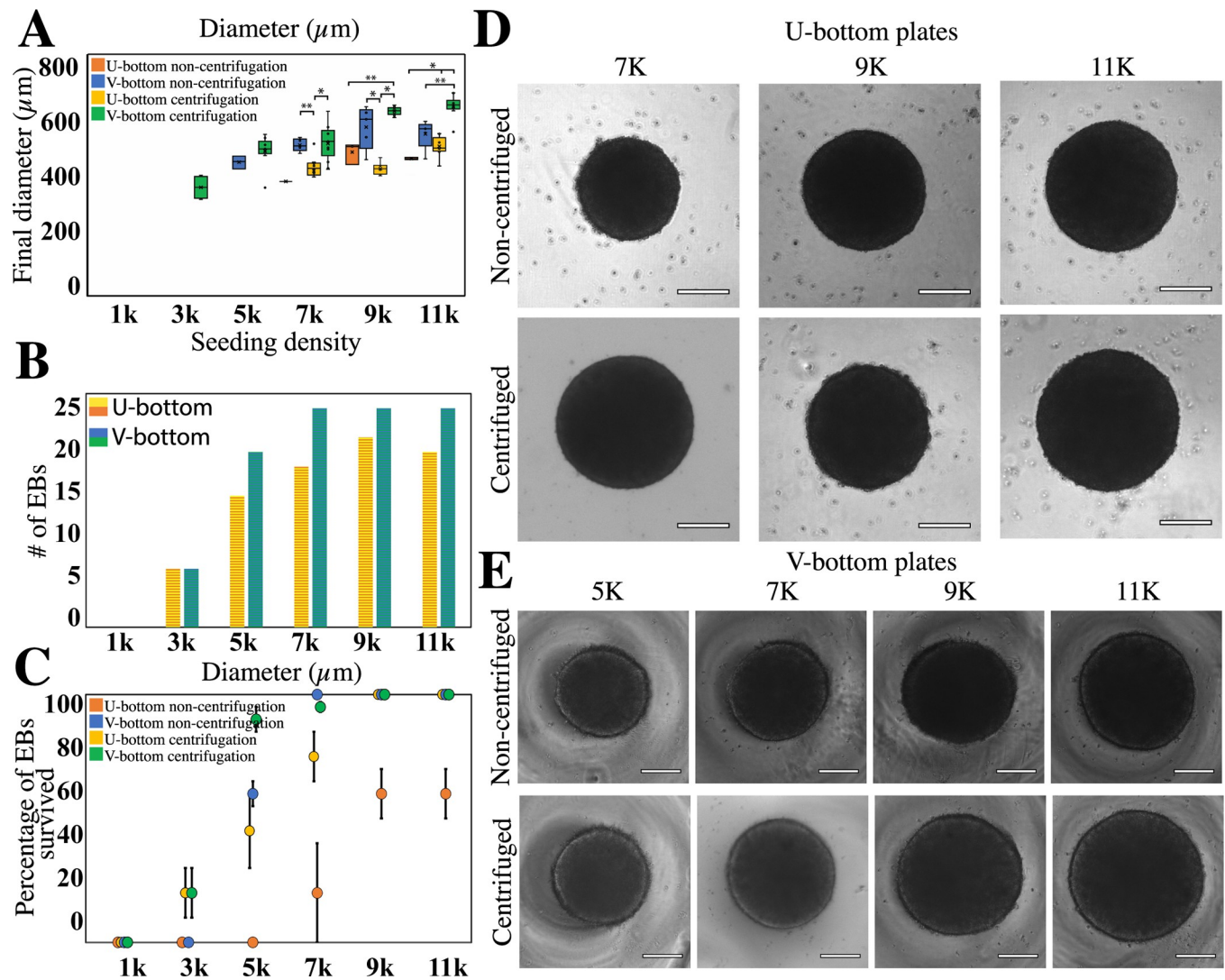


Fig 3. Diameter and survival of EBs fabricated under different conditions. (A) Box-plot distribution of the final diameter of EBs at different concentrations. Boxes are color coded to indicate the type of well plate and centrifugation treatment used. Box plots include the maximum, minimum, and mean values observed. A single asterisk (*) indicates a significant difference of $P < 0.001$. A double asterisk (**) indicates a significant difference of $P < 0.05$. We evaluated at least 5 EBs ($n = 5$) for each experimental group at the beginning of the experiment, and we conducted five independent experiments that included all treatments ($N = 5$). The distributions of the diameters of EBs produced in V-bottom and U-bottom wells. Average diameters were determined based on the number of EBs (n) that survived the entire culture time. (B) Histogram of EBs produced in U-bottom and V-bottom wells that survived until the end of the experiment. EBs formed in U-bottom wells are shown in blue; EBs formed in V-bottom wells are in orange. The initial number of EBs seeded = 25 in all experiments. (C) Percentages of the numbers of EBs that survived under the different fabrication conditions. (D,E) Brightfield images of spheroids formed at different fabrication conditions after 6 days of culture.

<https://doi.org/10.1371/journal.pone.0262062.g003>

centrifugation step, EB formation in U-bottom wells was feasible only at high seeding densities (i.e., equal or higher than 9×10^3 cells per well). Centrifugation enabled the formation of EBs in U-bottom wells at a wider range of seeding conditions, from 7×10^3 to 11×10^3 cells per well. This was an improvement on previously reported methods that identified 9×10^3 cells per well as a minimum threshold for reproducible EB formation [10, 30, 31].

Relevant indicators of the quality of the fabricated EBs were their final diameters and the span of their diameter dispersions. Previous research has shown that EBs with different diameters exhibit varying rates of differentiation or require different concentrations of induction factors to achieve homogeneous expression of differentiation genes [8, 32]. Reducing the variability of EB diameters may help to standardize subsequent organoid differentiation. Fig 3A shows the experimental conditions that enabled the formation of more homogeneous sets of EBs.

Some of the experimental conditions tested resulted in homogeneous sets of EBs that exhibited diameters with standard deviations of less than 50 μm , which is an improvement on the tolerance level previously reported [9, 10]. Indeed, the process of EB fabrication at high seeding densities (i.e., 9×10^3 and 11×10^3 cells per well) benefited greatly from the inclusion of a centrifugation step.

We also observed that EBs obtained using seeding densities of 9×10^3 and 11×10^3 cells per well did not differ significantly in their attributes (size and shape). This suggests the existence of an upper size threshold, of 640 μm in diameter, for the fabrication of EBs using V-bottom wells.

For example, EBs formed at high seeding densities in V-bottom plates exhibited a much lower dispersion in size with a centrifugation step than without. We also analyzed the sphericity (i.e., circularity and roundness) of the EBs formed under different fabrication conditions (Table 1). High values of EB circularity (i.e., above 0.8) resulted in size and shape homogeneity during subsequent culture and differentiation into organoids. We observed that our EBs had circularity exceeding 0.8 (Table 1), as reported previously for other EB protocols [33]. In general, the use of U- and V-bottom well plates did not affect EB circularity. The circularity was not significantly different at different cell seeding densities and remained constant throughout the culture.

We also conducted experiments in which we fabricated EBs using commercial ULA plates. These experiments enable the direct comparison of the most frequently used method used to produce EBs (fabrication in U-bottom ULA plates) [10, 12, 16, 21, 28, 34–40] versus our cost-effective methodology (see also S1 Table). In terms of size of the fabricated EBs, we did not

Table 1. Circularity and roundness, as determined by image analysis of embryoid bodies (EBs) cultured in V-bottom and U-bottom wells at different seeding densities. All values were calculated after 6 days of induction.

Seeding (cells/well)	V-bottom		U-bottom		V-bottom		U-bottom	
	no centrifugation		no centrifugation		centrifugation		centrifugation	
	Circularity	Roundness	Circularity	Roundness	Circularity	Roundness	Circularity	Roundness
1,000	-	-	-	-	-	-	-	-
3,000	-	-	-	-	0.88±0.013	0.93±0.03	-	-
5,000	0.87±0.024	0.88±0.04	-	-	0.88±0.007	0.95±0.02	-	-
7,000	0.88±0.011	0.92±0.03	0.89±0.001	0.98±0.02	0.88±0.011	0.92±0.03	0.89±0.005	0.92±0.06
9,000	0.88±0.008	0.96±0.01	0.89±0.001	0.97±0.02	0.88±0.012	0.95±0.02	0.89±0.003	0.96±0.05
11,000	0.88±0.008	0.92±0.01	0.90±0.001	0.98±0.01	0.89±0.009	0.97±0.01	0.89±0.004	0.9±0.06

*Values only provided if EB survived until Day 6.

<https://doi.org/10.1371/journal.pone.0262062.t001>

observe any significant differences between using regular U-bottom plates treated with anti-adherence solution or commercial U-bottom ULA plates (Fig 2C and 2D). However, EBs fabricated using V-bottom plates treated with anti-adherence solution were significantly larger than those fabricated using U-bottom ULA plates.

Effects of seeding density and geometry on EB survival

The survival of EBs differed depending on the fabrication conditions. Here, the term “survival” encompasses the maintenance of living cells and the retention of circularity, EB diameter, growth, and smooth edges (see S1C Fig. for exclusion criteria). Different cell seeding densities resulted in different percentages of EB survival. For both U-bottom and V-bottom wells, cell seeding densities of 1×10^3 and 3×10^3 cells per well did not yield viable EBs (Figs 2 and 3, and Table 1). This suggests that a minimal initial number of cells (i.e., $\sim 5 \times 10^3$ cells) is needed (in the absence of centrifugation) to promote adequate cell aggregation (Fig 3A, 3D and 3E) and EB survival (Fig 3B and 3C). This is in line with previously reported protocols that also indicated a minimum culture seeding of 5×10^3 cells for reproducible EB formation [41].

In general, we observed higher EB survival in V-bottom than in U-bottom wells (Fig 3B). For instance, in our experiments seeded at 5×10^3 cells per well, we only observed EB survival

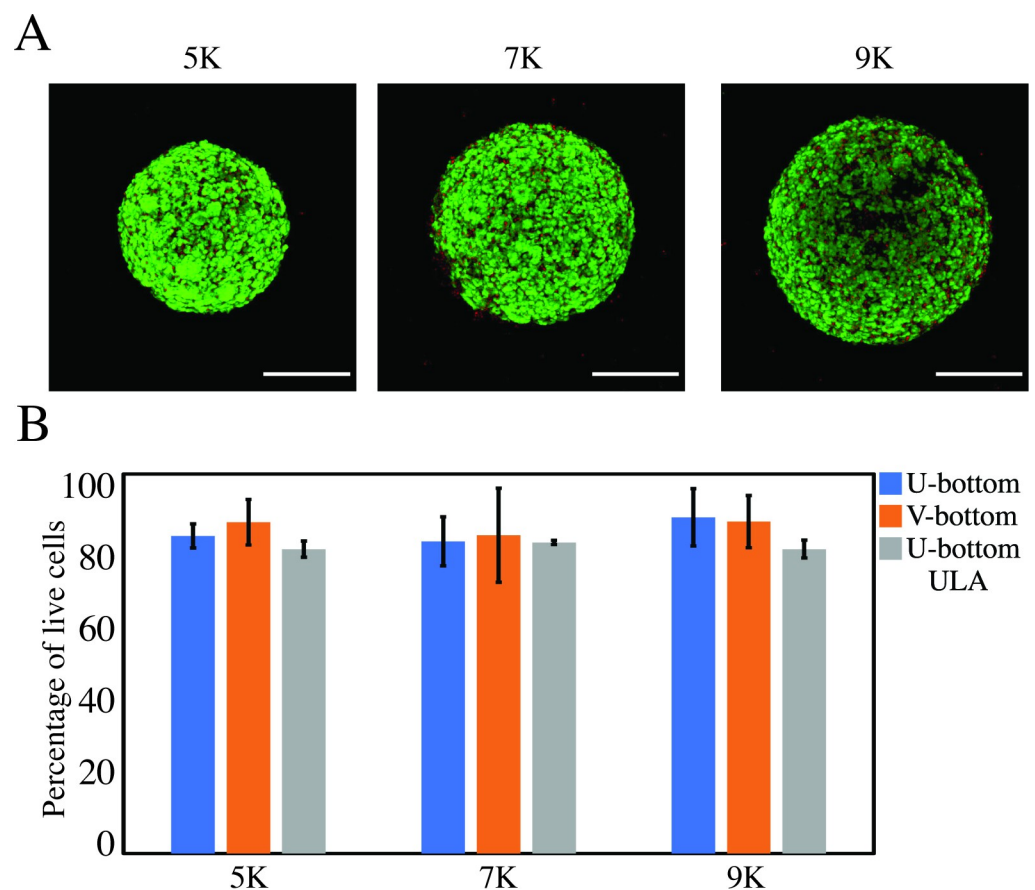


Fig 4. Cell viability in EBs fabricated using different methods. (A) Live/Dead assay conducted on EBs fabricated in U-bottom plates treated with anti-adherence solution, in V-bottom plates treated with anti-adherence solution, and in ULA plates. Calcein AM and ethidium homodimer-1 were used to stain live (green) and dead (red) cells, respectively. EBs were stained at day 6, before embedding in Matrigel for differentiation. Scale bar: 200 μ m. (B) EBs fabricated in ULA plates (control) and conventional U-bottom or V-bottom wells treated with anti-adherence solution exhibited statistically similar cell viabilities (>80%).

<https://doi.org/10.1371/journal.pone.0262062.g004>

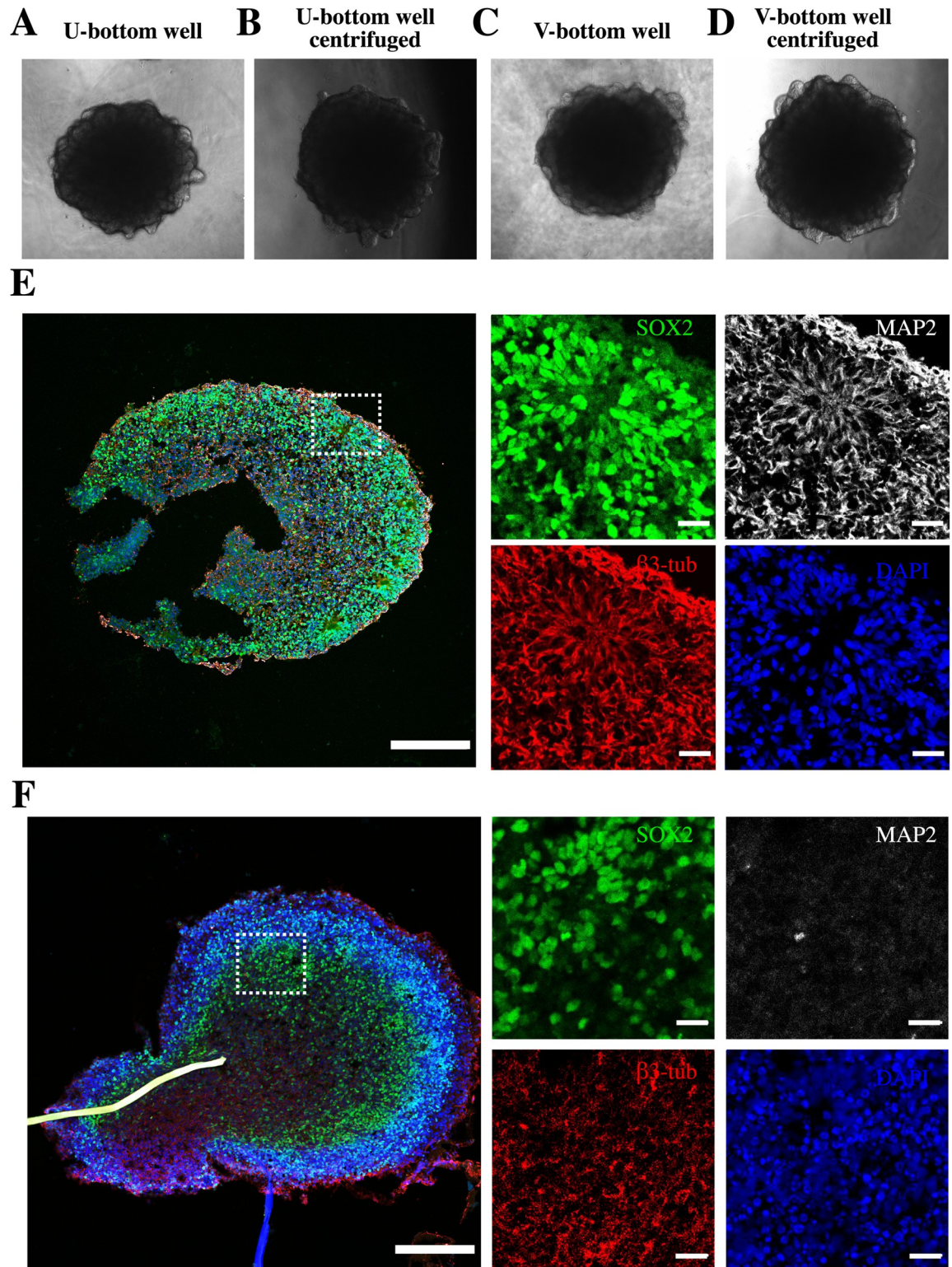


Fig 5. Examples of successful organoid differentiation from EBs. Brain organoids were formed using guided and unguided differentiation protocols to induce telencephalic differentiation. Regardless of the use of U- or V-bottom wells, the EBs demonstrated budding neuroepithelia at the periphery, hinting at successful organoid formation. Examples of EBs produced in a (A) a U-bottom well without centrifugation, (B) a U-bottom well with centrifugation, (C) a V-bottom well without centrifugation, and (D) a V-bottom well with centrifugation. Scale bar: 500 μ m. (E-F) Successful organoid differentiation at 30 days of culture. Dotted lines indicate the rosette

formations in the periphery of the organoid that show the undifferentiated neuroepithelial marker SOX2 and the neural identity markers of β 3-tubulin and MAP2. EBs cultured under (E) guided (F) and unguided differentiation protocols showed similar structural locations of the expressed markers, suggesting the neural predestination of the neuroepithelial tissue. (E) Guided protocols yielded a better-defined rosette and exhibited matured β -tubulin and MAP2 expression, while (F) the unguided protocols showed initial signs of axonal (β -tubulin) growth. Scale bar: 200 μ m.

<https://doi.org/10.1371/journal.pone.0262062.g005>

when V-bottom wells were used. EBs seeded in both U- and V-bottom wells exhibited similar initial diameters at 5×10^3 cell seeding. However, no EBs survived 6 days of culture in U-bottom wells, while EBs cultured in V-bottom plates had a survival rate of 60% ($n = 5$) (Fig 3C). Similarly, a 100% survival was observed in experiments in V-bottom wells seeded at 7×10^3 , 9×10^3 , and 11×10^3 cells per well, while the U-bottom wells yielded a 60% ($n = 5$) survival (Fig 3C). The discrepancy in survival between U-bottom and V-bottom wells at similar seeding densities (and initial diameters) reinforces the importance of well-plate geometry in its ability to aggregate cells and form EBs (Fig 3B and 3C). We also performed live/dead staining experiments to assess cell viability within the EBs. We found that, in surviving EBs, regardless of cell concentration, the percentage of viable cells remains above 80% after 6 days of culture (Fig 4A and 4B).

Previous experiments have shown the benefits of forced cell aggregation through centrifugation [14, 42]. Centrifugation of well plates clearly aids in precipitating cells together, increasing their aggregation (see also Fig 3D and 3E), cell-to-cell interactions, and survival. In our experiments, centrifugation immediately after cell seeding improved EB formation and survival at day 6, without affecting the initial EB diameter. EBs cultured in centrifuged V-bottom wells showed full (100%) survival at cell seeding densities of 7×10^3 K, 9×10^3 K, and 11×10^3 K cells per well (Fig 3C). At seeding densities of 5×10^3 K cells per well, survival was higher in centrifuged V-bottom wells than in non-centrifuged wells (90% versus 60%). Similarly, at seeding conditions of 5×10^3 K cells per well, EBs survival was higher in centrifuged U-bottom wells (i.e., 90%) than in non-centrifuged U-bottom wells (i.e., 20%). Our results suggest that centrifugation is an important step in this protocol, as it increases the survival percentage of EBs at medium seeding densities.

EB maturation into neural spheroids

We cultured EBs for extended time periods (i.e., more than 300 days) under guided [22] and unguided [43] differentiation protocols to induce them into telencephalic tissues and assess their functionality. All EBs formed in V-bottom and U-bottom wells showed budding tissue within the first couple of days of brain differentiation, which suggested their ability to develop into organoids once embedded into Matrigel (Fig 5). Unguided differentiation involved supplementing the medium with 20ng/mL of EGF and FGF-2, growth factors known to induced maturation to neurons if the neural identity was secured during the induction process [44]. Guided differentiation involved the use of enriched media added with WNT (CHIR99021) and bone morphogenic protein (BMP4) activators, to expedite the dorsalization of the tissue and induce proper neural tube formation [22].

We observed proper EB induction into neuroepithelia in guided and unguided differentiation experiments; both types of experiments yielded rosette lumens, formations only seen in the neuroectoderm, a neural tube analog [45]. All EBs fully developed into rosette forming organoids after 30 days of culture and expressed the undifferentiated neuroepithelial marker SOX2 and mature neuronal markers of β 3-Tubulin and MAP2 (Fig 5E and 5F). The abundant expression of SOX2 within these rosettes suggests the overall pluripotent nature of the tissue [46]. We observed lower expression of the MAP2+, an indicator of neuron maturity, in

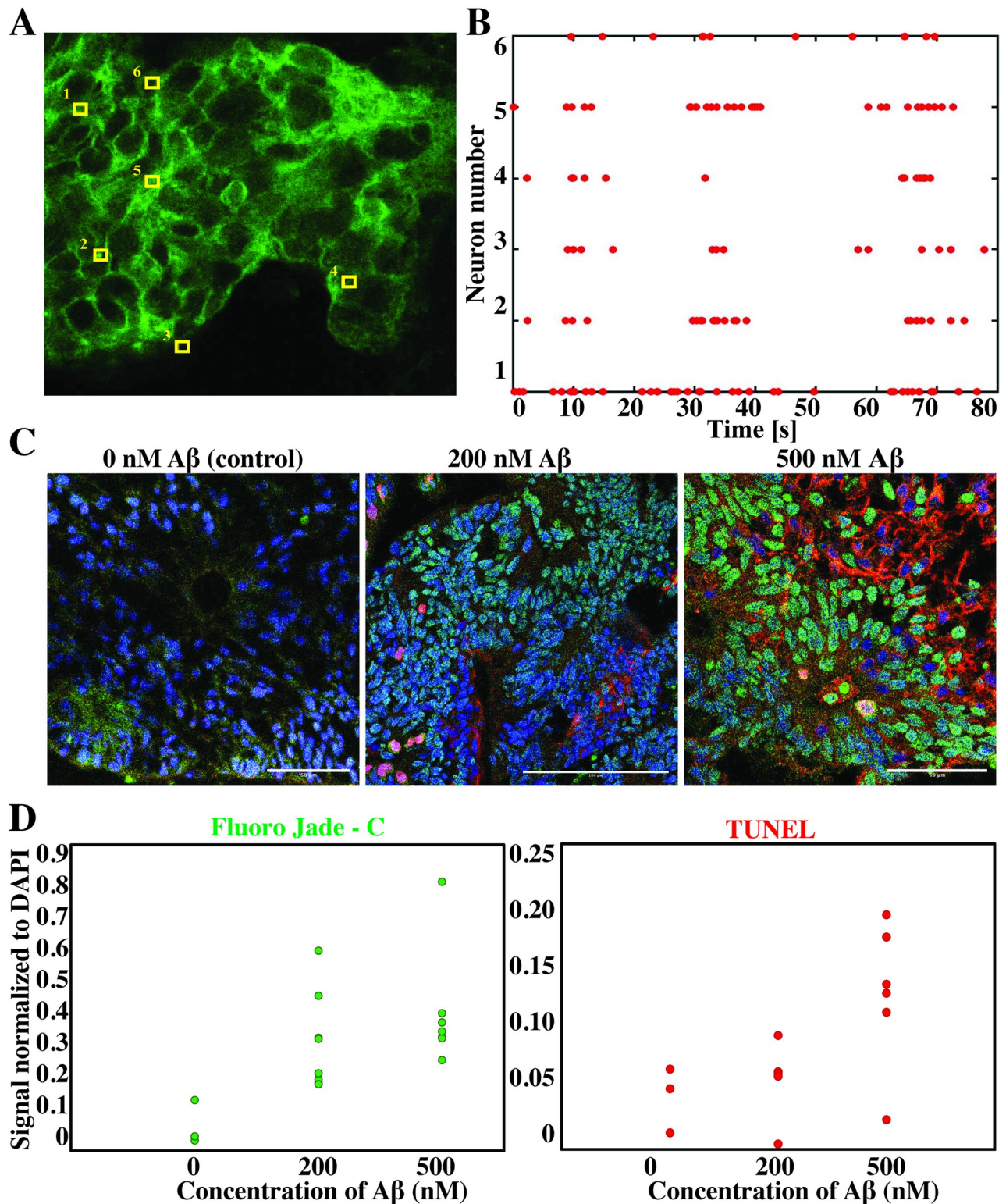


Fig 6. Functionality and possible applications of organoids derived from EBs. (A) Electrophysiological data were obtained using the voltage-sensitive FluoVolt dye. High resolution (10 ms) imaging of the measured area was used to identify individual neurons. (B) Raster plot of 6 individual neurons shown in (A) reveals frequent neuron firing and suggests synchronous activity at day 60. (C) Disease modeling was tested by exposing the organoids to 200 nM and 500 nM concentrations of soluble amyloid beta (A β). (D) Damage was assessed using the Fluoro Jade-C fluorescent marker (green) and (E) cell death with the BrdU TUNEL assay (red). Fluorescence images showed the location of the damage. Scale bar: 100 μ m. Quantification of the fluorescent image area normalized against the DAPI (blue) signal.

<https://doi.org/10.1371/journal.pone.0262062.g006>

organoids produced by unguided than in those generated in guided differentiation protocols (Fig 5F). Yet, the identical distribution of β 3-Tubulin and MAP2 in the outer rim of the rosette suggested [25] a successful induction into neuroepithelia even in unguided differentiation experiments.

The focus of this work is the production of EBs, and not the detailed description of the differentiation process of these EBs into organoids. Nevertheless, we considered that conducting proof-of-concept experiments was pertinent to demonstrate the functionality and usefulness of the organoids that can be differentiated from the EBs produced by the simple method reported here. Fig 6A and 6B show preliminary information derived from voltage-sensitive imaging that suggests that a capacity for synchronized neuron firing develops in the organoids after 60 days of culture. Fig 6C and 6D illustrate the use of organoids derived from the methods reported here in disease modeling experiments involving exposure to different concentrations of amyloid beta ($A\beta$). The organoids exhibited a dose-dependent response to $A\beta$, as evidenced by cell damage and cell death assays.

Conclusions

The combination of using standard V-bottom plates pretreated with a commercial anti-adherent solution 5 min before cell seeding, coupled with a brief centrifugation step after seeding, results in a cost-effective and reliable fabrication method for producing homogeneous and functional EBs.

Although V-bottom wells generated larger EBs than U-bottom wells, we also identified experimental conditions that would enable the reliable use of U-bottom wells for EB fabrication. The centrifugation of the well-plate cultures in V- and U-bottom well plates effectively enhanced the survival and reduced the size variability of neural EBs. In general, the standard deviation in the size of EBs generated with centrifugation was smaller than 50 μ m, which is lower than the reported variability using other protocols (i.e., 100 μ m) [9, 10].

Our method was standardized only for neuroepithelial EBs. However, we believe that it is translatable to the fabrication of a wide spectrum of organoids representative of different tissues. Many organoid cultures begin with circular EBs, including those related to kidney [27], liver [47], heart [48], optic cup [1], and other organs and tissues [46, 49]. The methods provided here could potentially facilitate and streamline organoid cultures in a diverse spectrum of labs spanning different fields. The protocols introduced here are simple and easily translatable to any cell culture laboratory. Their simplicity and cost-effectiveness may facilitate the entry of more laboratories into the nascent field of organoid fabrication and organoid-based research.

Supporting information

S1 Fig. Examples of properly or poorly formed EBs. Examples of appropriate EB growth in V-bottom (A) and U-bottom (B) anti-adherence coated plates at different days (“D”). Scale bar: 200 μ m. (C) Examples of EBs that fail to consolidate. (i) Low seeding concentrations or non-coated wells produce small cell aggregates. These small aggregates will not fuse together later and will not develop into EBs. Scale bar: 200 μ m. (ii) Central cluster with satellite aggregates in non-coated wells. As in (i), these peripheral aggregates will not fuse with the main cluster. Scale bar: 200 μ m. (iii) Disintegrated EB; remains of an EB that did not survive until the end of the experiment. Scale bar: 200 μ m.

(TIF)

S1 Table. Time and Cost comparison of different embryoid body well-plate formation techniques.

(DOCX)

Acknowledgments

We thank Carla Cofiño Fabres for providing V-bottom well plates. We also thank Mariana Garcia-Corral and Carla Annink for their support in cell culture techniques and standardization. We acknowledge the contribution of Joost Le Feber in the analysis of the electrophysiological data.

Author Contributions

Conceptualization: David Choy Buentello, Lena Sophie Koch, Mario Moisés Alvarez, Kerensa Broersen.

Data curation: Lena Sophie Koch, Mario Moisés Alvarez.

Formal analysis: David Choy Buentello, Lena Sophie Koch, Grissel Trujillo-de Santiago, Mario Moisés Alvarez, Kerensa Broersen.

Funding acquisition: Grissel Trujillo-de Santiago, Mario Moisés Alvarez, Kerensa Broersen.

Investigation: David Choy Buentello, Lena Sophie Koch.

Methodology: David Choy Buentello, Lena Sophie Koch, Kerensa Broersen.

Project administration: Grissel Trujillo-de Santiago, Kerensa Broersen.

Resources: Mario Moisés Alvarez, Kerensa Broersen.

Supervision: Grissel Trujillo-de Santiago, Mario Moisés Alvarez, Kerensa Broersen.

Visualization: David Choy Buentello.

Writing – original draft: David Choy Buentello, Mario Moisés Alvarez.

Writing – review & editing: Grissel Trujillo-de Santiago, Mario Moisés Alvarez, Kerensa Broersen.

References

1. Eiraku M, Takata N, Ishibashi H, Kawada M, Sakakura E, Okuda S, et al. Self-organizing optic-cup morphogenesis in three-dimensional culture. *Nature*. 2011; 472: 51–56. <https://doi.org/10.1038/nature09941> PMID: 21475194
2. Sato T, Vries RG, Snippert HJ, van de Wetering M, Barker N, Stange DE, et al. Single Lgr5 stem cells build crypt-villus structures in vitro without a mesenchymal niche. *Nature*. 2009; 459: 262–265. <https://doi.org/10.1038/nature07935> PMID: 19329995
3. Lancaster MA, Renner M, Martin C-A, Wenzel D, Bicknell LS, Hurles ME, et al. Cerebral organoids model human brain development and microcephaly. *Nature*. 2013; 501: 373–379. <https://doi.org/10.1038/nature12517> PMID: 23995685
4. Lancaster MA, Corsini NS, Wolfinger S, Gustafson EH, Phillips AW, Burkard TR, et al. Guided self-organization and cortical plate formation in human brain organoids. *Nat Biotechnol*. 2017; 35: 659–666. <https://doi.org/10.1038/nbt.3906> PMID: 28562594
5. Arora N, Alsous JI, Guggenheim JW, Mak M, Munera J, Wells JM, et al. A process engineering approach to increase organoid yield. *Development*. 2017; 144: 1128–1136. <https://doi.org/10.1242/dev.142919> PMID: 28174251
6. Leung BM, Leshner-Perez SC, Matsuoka T, Moraes C, Takayama S. Media additives to promote spheroid circularity and compactness in hanging drop platform. *Biomater Sci*. 2015; 3: 336–344. <https://doi.org/10.1039/c4bm00319e> PMID: 26218124

7. McMurtrey RJ. Analytic Models of Oxygen and Nutrient Diffusion, Metabolism Dynamics, and Architecture Optimization in Three-Dimensional Tissue Constructs with Applications and Insights in Cerebral Organoids. *Tissue Eng Part C Methods*. 2016; 22: 221–249. <https://doi.org/10.1089/ten.TEC.2015.0375> PMID: 26650970
8. Moon S-H, Ju J, Park S-J, Bae D, Chung H-M, Lee S-H. Optimizing human embryonic stem cells differentiation efficiency by screening size-tunable homogenous embryoid bodies. *Biomaterials*. 2014; 35: 5987–5997. <https://doi.org/10.1016/j.biomaterials.2014.04.001> PMID: 24780170
9. Douvaras P, Fossati V. Generation and isolation of oligodendrocyte progenitor cells from human pluripotent stem cells. *Nat Protoc*. 2015; 10: 1143–1154. <https://doi.org/10.1038/nprot.2015.075> PMID: 26134954
10. Lancaster MA, Knoblich JA. Generation of cerebral organoids from human pluripotent stem cells. *Nat Protoc*. 2014; 9: 2329–2340. <https://doi.org/10.1038/nprot.2014.158> PMID: 25188634
11. Rungarunlert S. Embryoid body formation from embryonic and induced pluripotent stem cells: Benefits of bioreactors. *World J Stem Cells*. 2009; 1: 11. <https://doi.org/10.4252/wjsc.v1.i1.11> PMID: 21607103
12. Das R, Fernandez JG. Additive manufacturing enables production of de novo cardiomyocytes by controlling embryoid body aggregation. *Bioprinting*. 2020; 20: e00091.
13. Chen C-S, Pegan J, Luna J, Xia B, McCloskey K, Chin W, et al. Shrinky-Dink Hanging Drops: A Simple Way to Form and Culture Embryoid Bodies. *J Vis Exp*. 2008; 13. <https://doi.org/10.3791/692> PMID: 19066572
14. Ungrin MD, Joshi C, Nica A, Bauwens C, Zandstra PW. Reproducible, Ultra High-Throughput Formation of Multicellular Organization from Single Cell Suspension-Derived Human Embryonic Stem Cell Aggregates. Callaerts P, editor. *PLoS One*. 2008; 3: e1565. <https://doi.org/10.1371/journal.pone.0001565> PMID: 18270562
15. Ezekiel UR, Muthuchamy M, Ryerse JS, Heuertz RM. Single embryoid body formation in a multi-well plate. *Electron J Biotechnol*. 2007; 10: 0–0.
16. Gao W, Wu D, Wang Y, Wang Z, Zou C, Dai Y, et al. Development of a novel and economical agar-based non-adherent three-dimensional culture method for enrichment of cancer stem-like cells. *Stem Cell Res Ther*. 2018; 9: 243. <https://doi.org/10.1186/s13287-018-0987-x> PMID: 30257704
17. Lam MT, Longaker MT. Comparison of several attachment methods for human iPS, embryonic and adipose-derived stem cells for tissue engineering. *J Tissue Eng Regen Med*. 2012; 6: s80–s86. <https://doi.org/10.1002/term.1499> PMID: 22610948
18. Tse JD, Moore R, Meng Y, Tao W, Smith ER, Xu XX. Dynamic conversion of cell sorting patterns in aggregates of embryonic stem cells with differential adhesive affinity. *BMC Dev Biol*. 2021; 21: 1–15. <https://doi.org/10.1186/s12861-020-00229-x> PMID: 33407089
19. Burridge PW, Anderson D, Priddle H, Barbadillo Muñoz MD, Chamberlain S, Allegrucci C, et al. Improved Human Embryonic Stem Cell Embryoid Body Homogeneity and Cardiomyocyte Differentiation from a Novel V-96 Plate Aggregation System Highlights Interline Variability. *Stem Cells*. 2007; 25: 929–938. <https://doi.org/10.1634/stemcells.2006-0598> PMID: 17185609
20. Camprostrini G, Meraviglia V, Giacomelli E, van Helden RWJ, Yiangou L, Davis RP, et al. Generation, functional analysis and applications of isogenic three-dimensional self-aggregating cardiac microtissues from human pluripotent stem cells. *Nat Protoc* 2021 164. 2021; 16: 2213–2256. <https://doi.org/10.1038/s41596-021-00497-2> PMID: 33772245
21. Muduli S, Chen L-H, Li M-P, Heish Z, Liu C-H, Kumar S, et al. Stem cell culture on polyvinyl alcohol hydrogels having different elasticity and immobilized with ECM-derived oligopeptides. *J Polym Eng*. 2017; 37: 647–660.
22. Sakaguchi H, Kadoshima T, Soen M, Narii N, Ishida Y, Ohgushi M, et al. Generation of functional hippocampal neurons from self-organizing human embryonic stem cell-derived dorsomedial telencephalic tissue. *Nat Commun*. 2015; 6: 8896. <https://doi.org/10.1038/ncomms9896> PMID: 26573335
23. Kuperstein I, Broersen K, Benilova I, Rozenski J, Jonckheere W, Debulpaep M, et al. Neurotoxicity of Alzheimer disease A β -peptides is induced by small changes in the A β 42 to A β 40 ratio Transaction Report. *EMBO J Peer Rev Process File-EMBO*. 2010. Available: <http://www.nature.com/emboj/about/process.html>
24. Xiang Y, Tanaka Y, Cakir B, Patterson B, Kim K-Y, Sun P, et al. hESC-Derived Thalamic Organoids Form Reciprocal Projections When Fused with Cortical Organoids. *Cell Stem Cell*. 2019; 24: 487–497. e7. <https://doi.org/10.1016/j.stem.2018.12.015> PMID: 30799279
25. Song L, Yuan X, Jones Z, Griffin K, Zhou Y, Ma T, et al. Assembly of Human Stem Cell-Derived Cortical Spheroids and Vascular Spheroids to Model 3-D Brain-like Tissues. *Sci Rep*. 2019; 9: 5977. <https://doi.org/10.1038/s41598-019-42439-9> PMID: 30979929

26. Ramirez S, Mukherjee A, Sepulveda S, Becerra-Calixto A, Bravo-Vasquez N, Gherardelli C, et al. Modeling Traumatic Brain Injury in Human Cerebral Organoids. *Cells*. 2021; 10: 2683. <https://doi.org/10.3390/cells10102683> PMID: 34685663
27. Sun G, Ding B, Wan M, Chen L, Jackson J, Atala A. Formation and optimization of three-dimensional organoids generated from urine-derived stem cells for renal function in vitro. *Stem Cell Res Ther*. 2020; 11: 309. <https://doi.org/10.1186/s13287-020-01822-4> PMID: 32698872
28. Burrig PW, Thompson S, Millrod MA, Weinberg S, Yuan X, Peters A, et al. A universal system for highly efficient cardiac differentiation of human induced pluripotent stem cells that eliminates interline variability. Pera M, editor. *PLoS One*. 2011; 6: e18293. <https://doi.org/10.1371/journal.pone.0018293> PMID: 21494607
29. Lee D, Pathak S, Jeong JH. Design and manufacture of 3D cell culture plate for mass production of cell-spheroids. *Sci Reports* 2019 91. 2019; 9: 1–8. <https://doi.org/10.1038/s41598-019-50186-0> PMID: 31562370
30. Bian S, Repic M, Guo Z, Kavirayani A, Burkard T, Bagley JA, et al. Genetically engineered cerebral organoids model brain tumor formation. *Nat Methods*. 2018; 15: 631–639. <https://doi.org/10.1038/s41592-018-0070-7> PMID: 30038414
31. Xiang Y, Cakir B, Park I-H. Generation of Regionally Specified Human Brain Organoids Resembling Thalamus Development. *STAR Protoc*. 2020; 1: 100001. <https://doi.org/10.1016/j.xpro.2019.100001> PMID: 33103124
32. Lee J, Lee S, Kim SM, Shin H. Size-controlled human adipose-derived stem cell spheroids hybridized with single-segmented nanofibers and their effect on viability and stem cell differentiation. *Biomater Res*. 2021; 25: 14. <https://doi.org/10.1186/s40824-021-00215-9> PMID: 33902733
33. Yoon S-JJ, Elahi LS, Paşca AM, Marton RM, Gordon A, Revah O, et al. Reliability of human cortical organoid generation. *Nat Methods*. 2019; 16: 75–78. <https://doi.org/10.1038/s41592-018-0255-0> PMID: 30573846
34. Phung YT, Barbone D, Broaddus VC, Ho M. Rapid Generation of In Vitro Multicellular Spheroids for the Study of Monoclonal Antibody Therapy. *J Cancer*. 2011; 2: 507–514. <https://doi.org/10.7150/jca.2.507> PMID: 22043235
35. Garcia-Alegria E, Potts B, Menegatti S, Kouskoff V. In vitro differentiation of human embryonic stem cells to hemogenic endothelium and blood progenitors via embryoid body formation. *STAR Protoc*. 2021; 2: 100367. <https://doi.org/10.1016/j.xpro.2021.100367> PMID: 33718891
36. Pettinato G, Wen X, Zhang N. Engineering Strategies for the Formation of Embryoid Bodies from Human Pluripotent Stem Cells. *Stem Cells Dev*. 2015; 24: 1595–1609. <https://doi.org/10.1089/scd.2014.0427> PMID: 25900308
37. Choi YY, Chung BG, Lee DH, Khademhosseini A, Kim J-H, Lee S-H. Controlled-size embryoid body formation in concave microwell arrays. *Biomaterials*. 2010; 31: 4296–4303. <https://doi.org/10.1016/j.biomaterials.2010.01.115> PMID: 20206991
38. Perez JE, Nagle I, Wilhelm C. Magnetic molding of tumor spheroids: emerging model for cancer screening. *Biofabrication*. 2021; 13: 015018.
39. Ka Turnovcova, Marevoka D, Sursal T, Krupova M, Gandhi R, Krupa P, et al. Understanding the Biological Basis of Glioblastoma Patient-derived Spheroids. *Anticancer Res*. 2021; 41: 1183–1195. <https://doi.org/10.21873/anticancerres.14875> PMID: 33788709
40. Ouyang L, Yao R, Mao S, Chen X, Na J, Sun W. Three-dimensional bioprinting of embryonic stem cells directs highly uniform embryoid body formation. *Biofabrication*. 2015; 7: 044101. <https://doi.org/10.1088/1758-5090/7/4/044101> PMID: 26531008
41. Yakoub AM, Sadek M. Development and Characterization of Human Cerebral Organoids. *Cell Transplant*. 2018; 27: 393–406. <https://doi.org/10.1177/0963689717752946> PMID: 29749250
42. Ng ES, Davis RP, Azzola L, Stanley EG, Elefanty AG. Forced aggregation of defined numbers of human embryonic stem cells into embryoid bodies fosters robust, reproducible hematopoietic differentiation. *Blood*. 2005; 106: 1601–1603. <https://doi.org/10.1182/blood-2005-03-0987> PMID: 15914555
43. Birey F, Andersen J, Makinson CD, Islam S, Wei W, Huber N, et al. Assembly of functionally integrated human forebrain spheroids. *Nature*. 2017; 545: 54–59. <https://doi.org/10.1038/nature22330> PMID: 28445465
44. Ciccolini F, Svendsen CN. Fibroblast Growth Factor 2 (FGF-2) Promotes Acquisition of Epidermal Growth Factor (EGF) Responsiveness in Mouse Striatum Precursor Cells: Identification of Neural Precursors Responding to both EGF and FGF-2. *J Neurosci*. 1998; 18: 7869–7880. <https://doi.org/10.1523/JNEUROSCI.18-19-07869.1998> PMID: 9742155

45. Wilson PG, Stice SS. Development and differentiation of neural rosettes derived from human embryonic stem cells. *Stem Cell Rev.* 2006; 2: 67–77. <https://doi.org/10.1007/s12015-006-0011-1> PMID: [17142889](https://pubmed.ncbi.nlm.nih.gov/17142889/)
46. Turner DA, Baillie-Johnson P, Martinez Arias A. Organoids and the genetically encoded self-assembly of embryonic stem cells. *BioEssays.* 2016; 38: 181–191. <https://doi.org/10.1002/bies.201500111> PMID: [26666846](https://pubmed.ncbi.nlm.nih.gov/26666846/)
47. Angireddy R, Chowdhury AR, Zielonka J, Ruthel G, Kalyanaraman B, Avadhani NG. Alcohol-induced CYP2E1, mitochondrial dynamics and retrograde signaling in human hepatic 3D organoids. *Free Radic Biol Med.* 2020; 159: 1–14. <https://doi.org/10.1016/j.freeradbiomed.2020.06.030> PMID: [32738395](https://pubmed.ncbi.nlm.nih.gov/32738395/)
48. Helms HR, Jarrell DK, Jacot JG. Generation of Cardiac Organoids Using Cardiomyocytes, Endothelial Cells, Epicardial Cells, and Cardiac Fibroblasts Derived From Human Induced Pluripotent Stem Cells. *FASEB J.* 2019; 33: lb170–lb170.
49. Brassard JA, Lutolf MP. Engineering Stem Cell Self-organization to Build Better Organoids. *Cell Stem Cell.* 2019; 24: 860–876. <https://doi.org/10.1016/j.stem.2019.05.005> PMID: [31173716](https://pubmed.ncbi.nlm.nih.gov/31173716/)